Cell Number and Neuropil Alterations in Subregions of the Anterior Hippocampus in a Female Monkey Model of Depression

Supplemental Information

Supplemental Methods and Materials

Subjects

The animals were housed under a 12/12 light/dark cycle. At the completion of the parent study (published in references 1-3), all 28 animals were euthanized with sodium pentobarbital in accordance with guidelines established by the American Veterinary Medical Association, as previously described (2).

Social Status and Behavioral Depression

Across our studies, approximately 60% of socially subordinate and 10% of socially dominant females engage in depressive behavior, thus social status and depressive behavior are two separate, yet related, constructs (for reviews, see 4, 5).

Tissue Preparation and Cell Labeling

At necropsy, hemisected brains were rapidly removed, frozen and stored at -80°C. The temporal lobe from one hemisphere of each animal was dissected at -20°C, immersion-fixed in 4% phosphate-buffered paraformaldehyde at 4°C for one week, and then cryoprotected in graded concentrations of phosphate-buffered sucrose (up to 30%). Fixed-tissue blocks were frozen in TFM™ (TBS®, Inc., Durham, NC) and coronally cryosectioned at 50 µm throughout the anterior-posterior extent of the hippocampus. Tissue sections were collected into antifreeze solution (1:1:2 ethylene glycol, glycerol and 0.1M phosphate-buffered saline) and stored at

-20ºC until use. To control for laterality effects, experimental groups were counterbalanced for hemisphere as in previous hippocampal volumetry studies (6).

Immunohistochemistry and Histology

NeuN immunohistochemistry was used to visualize pyramidal neurons (Figure 2A). Sections were processed in batches equally representing behavioral depression status. Sections were washed of antifreeze solution in 0.1M tris-buffered saline (TBS), pH 7.5, and endogenous peroxidase activity was reduced by incubation for 30 minutes in 0.6% hydrogen peroxide diluted in TBS. Sections were washed and incubated for 1 hour at room temperature in TBS containing 5% normal horse serum and 0.2% Triton X-100 followed by overnight incubation in the same solution at 4ºC containing mouse monoclonal anti-NeuN (1:20,000; MAB377, Millipore, Billerica, MA). Label was detected with biotinylated anti-mouse secondary antibody (1:1000; Vector Laboratories, Inc., Burlingame, CA) and visualized employing peroxidase-conjugated avidin-biotin complex (ABC Elite Kit, Vector Laboratories, Inc.) and nickel enhanced diaminobenzidine peroxidase substrate (DAB Kit, Vector Laboratories, Inc). Sections were mounted in TBS onto superfrost Plus slides (Fisher Scientific, Pittsburgh, PA), blotted of residual buffer, air dried 30 minutes, dehydrated using a graded series of ethanol, cleared in xylene and coverslipped using Cytoseal 60 permanent mounting medium (VWR, West Chester, PA).

Histochemistry for Nissl substance was used to label granule neurons and glia. NeuN staining was weak with cells barely discernible in the center thickness of the tissue at the level of the dentate gyrus granule cell layer (Figure 2B-D), presumably due to the high packing density of neurons in this cell layer and the large section thickness (50 µm) necessary for stereological analysis, as described above. Available glial markers, such as GFAP and S100β for astrocytes, are known to be up- or down-regulated by various disease states and may not be expressed at detectable levels reliably by all astrocytes in healthy tissue (7, 8, 9), making them

unreliable for determining cell type-specific numbers. Thus, standard Nissl substance staining with cresyl violet was used to visualize all glial cells without regard to glial subtype, as well as granule neurons (Figure 2C-D). Sections were washed of antifreeze solution in TBS, mounted onto superfrost Plus slides, blotted of residual buffer, and air dried 60 minutes. Slide-mounted sections were dehydrated using a graded series of ethanol, cleared in xylene, rehydrated through a graded series of ethanol, and stained with 0.1% cresyl violet acetate for two minutes. Sections were then dehydrated/differentiated through a series of graded ethanol, cleared in xylene and coverslipped using Cytoseal 60 permanent mounting medium.

Quantitative Stereological Analyses

This tissue sectioning thickness of 50 µm was necessary for proper stereological analysis. Briefly, tissue staining and dehydration reduces the tissue thickness by approximately 60% to 20 µm. To reduce the possibility of including cells that were sheared during sectioning, the upper and lower guard height was set at 3 µm, reducing the possible dissector height to 14 µm. Objects of interest were only counted as they came into focus within the dissector height. In this study, a height of 10 µm was required to account for the size of the objects being counted (e.g. pyramidal neurons).

The borders of all regions of interest (ROIs) within each section were defined at one sitting (10X objective). NeuN-immunoreactive pyramidal neurons were evaluated using a plan-fluorite 40X (N.A. = 1.3) oil immersion objective given their large size and disperse distribution within the pyramidal cell layers (Figure S2A). Cresyl-violet stained granule neurons were evaluated using a plan-apochromat 60X (N.A. = 1.4) oil immersion objective given their small size and high packing density. All glial cells were counted regardless of subtype and were distinguished from neurons under 60X magnification by their smaller size and lack of a prominent nucleolus (Figure S2C). Cells were quantified in counting frames within sampling grids (area, A, of x and y steps) distributed in a systematically random manner, and visualized

by focusing through the dissector height (h), below the guard height of 3 µm, and inside the counting frame area, A(frame). Section thickness (t) was measured in every third counting frame. The total number of cells for each ROI was estimated as $N = \Sigma Q^{-} \times 1/ssf \times 1/asf \times 1/tsf$, where ΣQ^{-} is the total number of objects counted within an ROI across all sections, ssf (section sampling fraction) is the section sampling interval, asf (area sampling fraction) = A(frame) / A(x,y steps), and tsf (thickness sampling fraction) = h/t.

Table S1. Stereological Parameters

Region/Object	ssf	A(frame) (µm × µm)	A(x,y step) (µm × µm)	h (µm)	T[a] (µm)	ΣQ[-] [a]	CE[a,b]
Anterior hippocampus							
Dentate gyrus							
Granule neurons	1/12	20 × 20	225 × 225	10	20.0 ± 0.23	487 ± 43	0.047
Glia	1/12	50 × 50	450 × 450	10	21.5 ± 0.26	549 ± 39	0.044
Proximal CA3							
Pyramidal neurons	1/12	70 × 70	350 × 350	10	16.3 ± 0.23	272 ± 16	0.062
Glia	1/12	50 × 50	400 × 400	10	22.0 ± 0.22	407 ± 24	0.051
Distal CA3/CA2							
Pyramidal neurons	1/12	70 × 70	350 × 350	10	16.4 ± 0.22	461 ± 18	0.047
Glia	1/12	50 × 50	400 × 400	10	22.4 ± 0.24	1138 ± 66	0.030
CA1/subiculum							
Pyramidal neurons	1/12	70 × 70	500 × 500	10	17.0 ± 0.26	522 ± 20	0.044
Glia	1/12	50 × 50	650 × 650	10	22.5 ± 0.25	602 ± 40	0.042
Posterior hippocampus							
Dentate gyrus							
Granule Neurons	1/24	20 × 20	225 × 225	10	20.2 ± 0.26	435 ± 34	0.050
Glia	1/24	50 × 50	450 × 450	10	20.8 ± 0.29	402 ± 20	0.051
Proximal CA3							
Pyramidal neurons	1/24	70 × 70	350 × 350	10	18.3 ± 0.52	215 ± 14	0.071
Glia	1/24	50 × 50	400 × 400	10	21.1 ± 0.27	215 ± 13	0.070
Distal CA3/CA2							
Pyramidal neurons	1/24	70 × 70	350 × 350	10	17.8 ± 0.43	390 ± 21	0.051
Glia	1/24	50 × 50	400 × 400	10	21.8 ± 0.27	540 ± 25	0.044
CA1/subiculum							
Pyramidal neurons	1/24	70 × 70	500 × 500	10	17.6 ± 0.47	450 ± 17	0.047
Glia	1/24	50 × 50	650 × 650	10	21.7 ± 0.32	407 ± 16	0.050

[a]Values listed are means ± SEMs.
[b]For all mean CE (coefficient of error), SEM was ≤0.003.
ssf: section sampling fraction; A(frame): area of counting frame; A(x,y steps): area of sampling grid; h: height of dissector; t: section thickness; ΣN^-: number of objects counted.

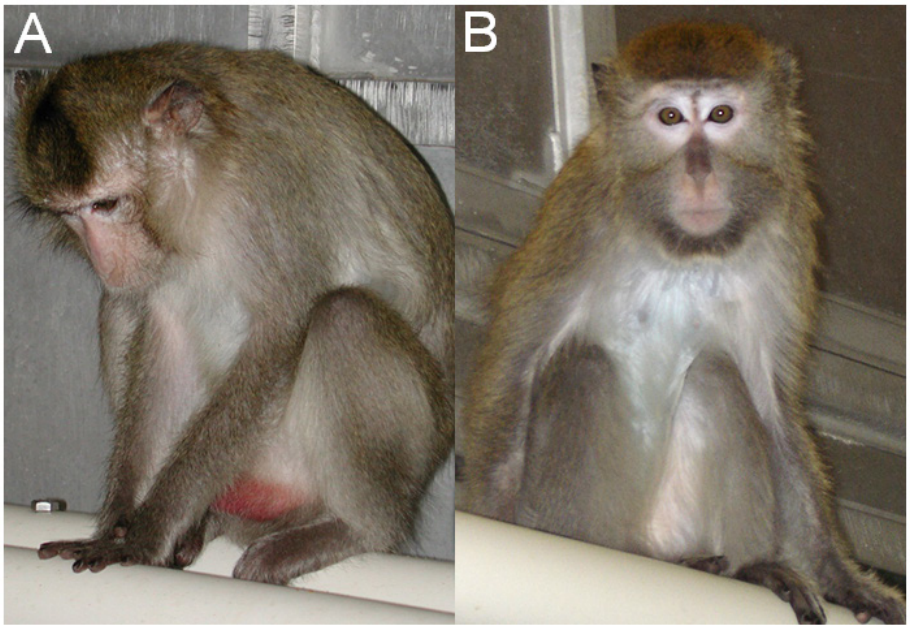

Figure S1. Monkeys displaying depressed **(A)** and nondepressed behavior **(B)**. The monkey displaying depressive behavior **(A)** appears inattentive, and is in a slumped body posture (head below shoulders), with eyes open and directed downward. The monkey displaying nondepressed behavior **(B)** is alert and attentive to the photographer.

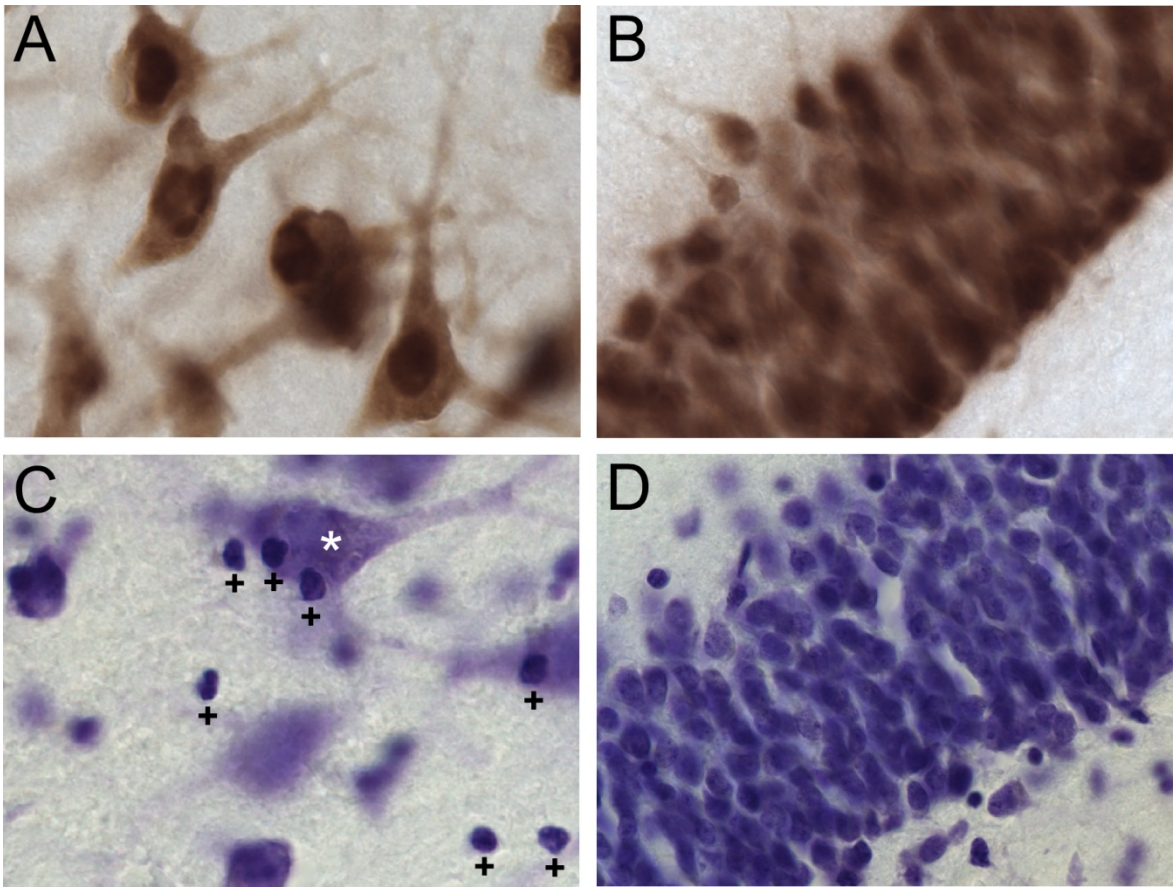

Figure S2. NeuN and cresyl violet were used to visualize cells. **(A)** NeuN-immunoreactive pyramidal neurons were clearly labeled through the extent of the tissue. **(B)** Weak NeuN staining was observed in the densely-packed granule cell layer toward the center of the 50 µm sections. **(C)** Glial cells stained with cresyl violet were easily distinguished from neurons and endothelial cells based on distinct, known morphological characteristics. White asterisks indicate neurons and black plus signs indicate glial cells. **(D)** Unlike NeuN, histological staining with cresyl violet clearly delineated granule neurons in the center thickness of the tissue section. Magnification: 60X.

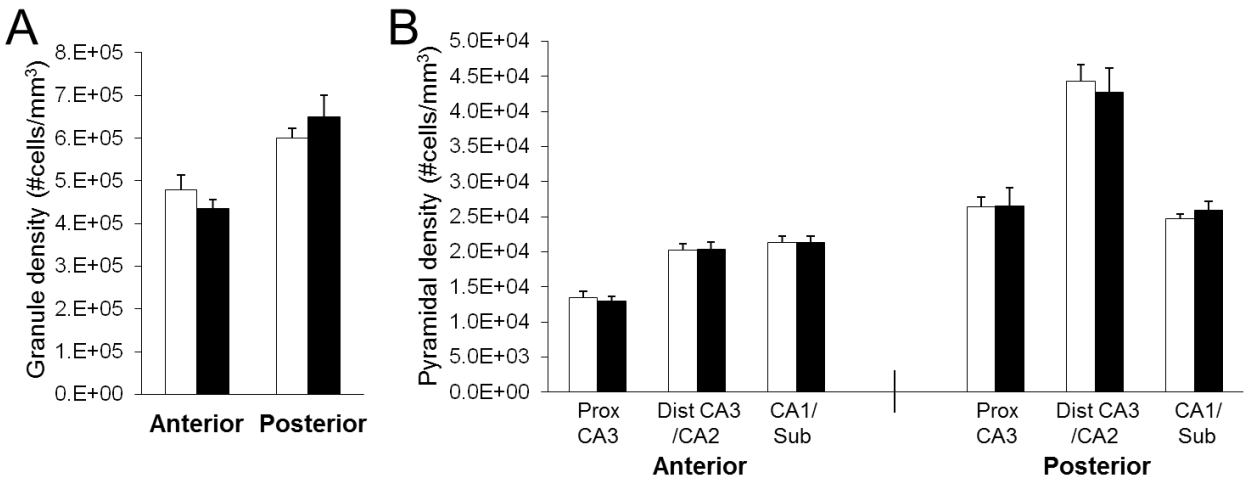

Figure S3. Neuronal density is unaltered in behaviorally depressed female monkeys. **(A-B)** No significant effects were observed for neuronal density in the anterior (main: $F_{(1,14)} = 1.03$, $p = 0.33$; interaction: $F_{(3,42)} = 1.05$, $p = 0.38$) or posterior (main: $F_{(1,14)} = 0.77$, $p = 0.39$; interaction: $F_{(3,42)} = 0.86$, $p = 0.47$) hippocampus.

Supplemental References

1. Shively CA, Register TC, Friedman DP, Morgan TM, Thompson J, Lanier T (2005): Social stress-associated depression in adult female cynomolgus monkeys (Macaca fascicularis). *Biol Psychol* 69: 67-84.
2. Shively CA, Register TC, Adams MR, Golden DL, Willard SL, Clarkson TB (2008): Depressive behavior and coronary artery atherogenesis in adult female cynomolgus monkeys. *Psychosom Med* 70: 637-645.
3. Shively CA, Mussselman DL, Willard SL (2009): Stress, depression, and coronary artery disease: Modeling comorbidity in female primates. *Neurosci Biobehav Rev* 33: 133-144.
4. Willard SL, Shively CA. (2012): Modeling depression in adult female cynomolgus monkeys (Macaca fascicularis). *Am J Primatol* 74: 528-542.
5. Shively CA, Willard SL (2012): Behavioral and neurobiological characteristics of social stress versus depression in nonhuman primates. *Exp Neurol* 233: 87-94.
6. Willard SL, Friedman DP, Henkel CK, Shively CA (2009): Anterior hippocampal volume is reduced in behaviorally depressed female cynomolgus macaques. *Psychoneuroendocrinology* 34: 1469-1475.
7. Gosselin RD, Gibney S, O'Malley D, Dinan TG, Cryan JF (2009): Region specific decrease in glial fibrillary acidic protein immunoreactivity in the brain of a rat model of depression. *Neuroscience* 159: 915-925.
8. Middeldorp J, Hol EM (2011): GFAP in health and disease. *Prog Neurobiol* 93: 421-443.
9. Sofroniew MV, Vinters HV (2010): Astrocytes: biology and pathology. *Acta Neuropathol* 119: 7-35.